

XPAL modeling and theory

Andrew D. Palla^a, David L. Carroll^a, Joseph T. Verdeyen^a, and Michael C. Heaven^b

^aCU Aerospace, Urbana, IL 61820

^bEmory University, Atlanta, GA 30322

ABSTRACT

The exciplex pumped alkali laser (XPAL) system has been demonstrated in mixtures of Cs vapor, Ar, with and without ethane, by pumping Cs-Ar atomic collision pairs and subsequent dissociation of diatomic, electronically-excited CsAr molecules (exciplexes or excimers). The blue satellites of the alkali D₂ lines provide an advantageous pathway for optically pumping atomic alkali lasers on the principal series (resonance) transitions with broad linewidth (>2 nm) semiconductor diode lasers. Because of the addition of atomic collision pairs and exciplex states, modeling of the XPAL system is more complicated than classic diode pumped alkali laser (DPAL) modeling. The BLAZE-V model is utilized for high-fidelity simulations. BLAZE-V is a time-dependent finite-volume model including transport, thermal, and kinetic effects appropriate for the simulation of a cylindrical closed cell XPAL system. The model is also regularly used for flowing gas laser simulations and is easily adapted for DPAL. High fidelity calculations of pulsed XPAL operation as a function of temperature and pressure are presented along with a theoretical analysis of requirements for optical transparency in XPAL systems. The detailed modeling predicts higher XPAL performance as the rare gas pressure increases, and that higher output powers are obtainable with higher temperature. The theoretical model indicates that the choice of alkali and rare gas mixture can significantly impact the required intensities for optical transparency.

Keywords: exciplex pumped alkali laser, XPAL, diode pumped alkali laser, DPAL, excimer

1. INTRODUCTION

Approximately eight years ago, Krupke *et al.* [Krupke, 2003] demonstrated an optically-pumped atomic Rb laser operating on the resonance line at 795 nm. This scheme is commonly referred to as a diode pumped alkali laser (DPAL), and an equivalent pictorial representation for the Cs version of DPAL is illustrated in Fig. 1. Several other important studies followed the initial DPAL demonstration including theoretical modeling [Beach, 2004; Hager, 2010; Komashko, 2010], demonstration of lasing with other alkalis [Beach, 2004; Zhdanov, 2007a], lasing with helium as the ²P_{3/2}→²P_{1/2} relaxer gas rather than ethane [Zhdanov, 2007b; Zweiback, 2009], a multi-diode pump scheme has produced 48 W of output power at 894 nm [Zhdanov, 2008], and a high power diode stack has produced an average output power of 145 W at 794 nm [Zweiback, 2010]. The level of interest in the laser community is rising rapidly because it appears that this laser may offer a route to extremely high power levels. The primary reason for the interest is that it allows one to use high power semiconductor laser diodes as the pump source to drive a gas laser.

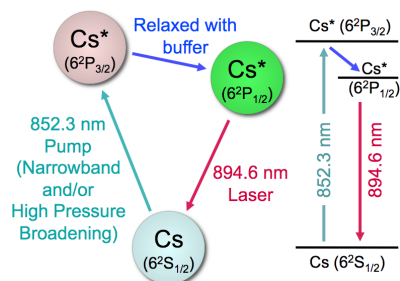


Figure 1. Pictorial representation of the DPAL scheme for pumping the cesium $Cs(6^2P_{3/2})$ state, resulting in lasing on the $Cs(6^2P_{1/2}) \rightarrow Cs(6^2S_{1/2})$ transition at 894.6 nm (in vacuum, 894.3 nm in air).

All of this is quite attractive but the basic DPAL pumping scheme has some drawbacks. Because the atomic transition that is being pumped is spectrally very narrow (≈ 10 GHz, or equivalently ≈ 0.02 nm), only a limited portion of the semiconductor laser power will be absorbed by the alkali vapor because common semiconductor lasers typically emit with spectral widths of > 1000 GHz (roughly 2 nm). To surmount this difficulty, Krupke *et al.* [Krupke, 2004] proposed adding He gas (or other gas) to broaden the linewidth of the transition. Unfortunately, to do this with He (which has a pressure broadening coefficient of approximately 20 GHz/atm at a wavelength of 800 nm), one must add up to 25-50 atmospheres (19,000-38,000 Torr) of gas if the pump transition linewidth is to match the spectral breadth of the semiconductor laser [Krupke, 2004; Beach, 2004]. One alternative is to narrow the linewidth of the pump laser. While significant advances have been made in this area [Podvyaznyy, 2010], this approach dramatically increases the cost, and

scaling of such narrow linewidth diode stacks to very high power is still uncertain. A phenomenon which appears to have some benefits for this problem is pump wave bleaching [Hager, 2010; Komashko, 2010], however it is not yet clear to what extent this phenomenon will alleviate the problem of uniform pumping of the gain medium in a DPAL system.

The XPAL approach takes a different course to this problem by invoking a molecular interaction to allow us to pump away from the atomic resonance but still obtain efficient lasing from the atom itself. Consider, for example, the CsAr molecule. It has been known for three decades [Hedges, 1972; Chen and Phelps, 1973] that the interaction of Cs and Ar atoms forms collision pairs that can absorb photons to create exciplexes (or excimers). The result is that mixtures of Cs vapors and Ar gas exhibit strong absorption tens of Å (several nm) away from the atomic resonance. Figure 2 illustrates the differences in transmission (or equivalently absorption) for a Cs cell filled with 480 Torr of He at 110°C that relies on Lorentzian broadening to absorb the pump radiation versus a Cs cell filled with 600 Torr of Ar at 200°C which has a considerably broader absorption spectrum due to the blue and red wings from the exciplex. It is clear from Fig. 2 that the cell relying only on Lorentzian absorption will have a difficult time absorbing the pump radiation from a high-efficiency, broadband (≈ 2 nm) diode laser source, whereas absorbing the pump radiation in the exciplex wings can be easily accommodated. For conceptual clarity, Cs-Ar interaction potentials including illustrations of the two Cs-Ar XPAL system pumping pathways and the four- and five-level laser operation mechanisms are shown in Fig. 3. The four- and five-level laser operation mechanisms are further illustrated in Fig. 4.

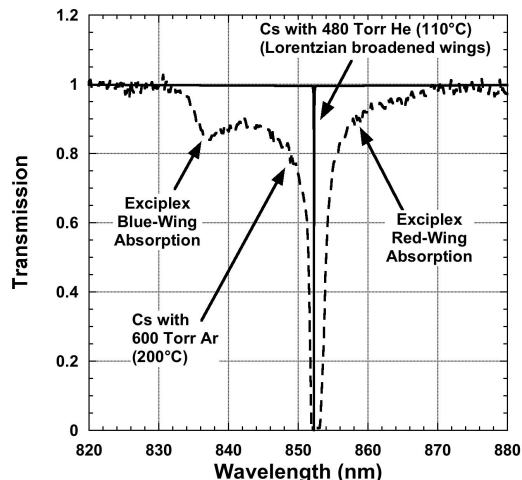


Figure 2. Transmission traces of Cs-He (480 Torr) with Lorentzian line broadening at 110°C and Cs-Ar (600 Torr) with exciplex blue- and red-wing broadening taken at 200°C. The broadband exciplex absorption is clearly broad enough to accept the pump radiation from broadband (≈ 2 nm) high eff. laser diodes, whereas the Lorentzian broadened line is only ≈ 0.03 nm in width.

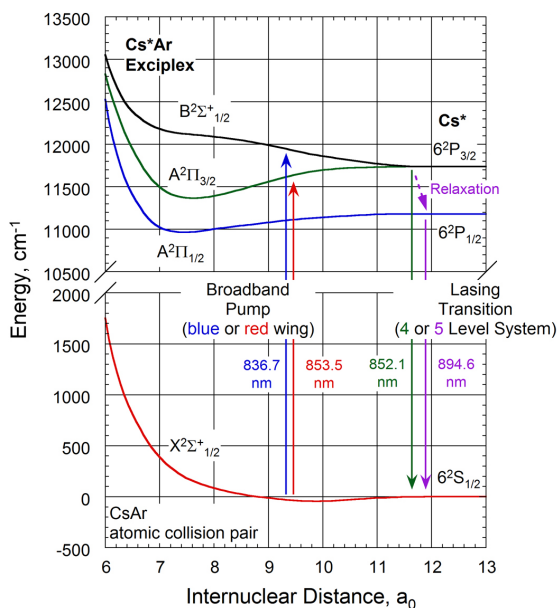


Figure 3. Interaction potentials of Cs-Ar. The arrows indicate the various pumping pathways, with two variations of the XPAL scheme shown. Laser action at 852.1 nm and 894.3 nm correspond to four- and five-level operation respectively.

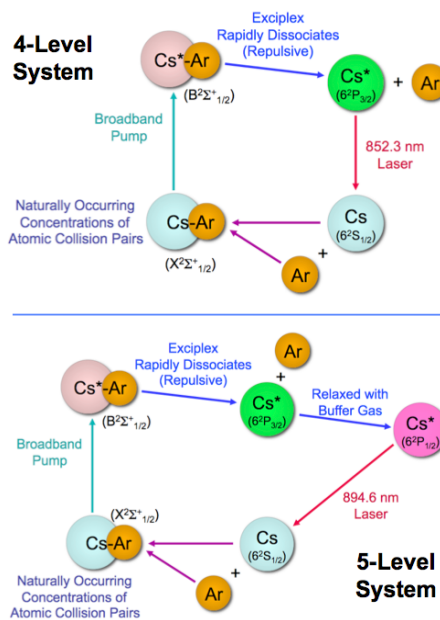
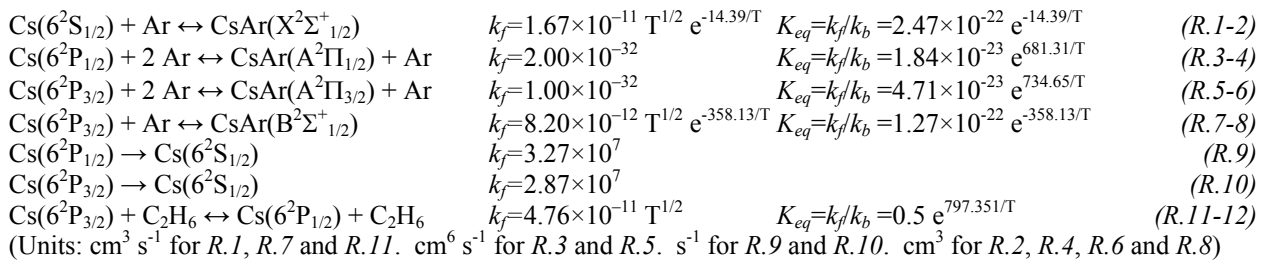


Figure 4. Pictorial representations of four- and five-level XPAL operation respectively using either pumping pathway.

The exciplex pumped alkali laser (XPAL) system was demonstrated by Readle *et al.* [Readle 2008, 2009a-b, 2010a-b] in mixtures of Cs vapor, Ar, and ethane, by pumping Cs-Ar atomic collision pairs and subsequent dissociation of diatomic, electronically-excited CsAr molecules (exciplexes or excimers). The four- and five-level variations of the pulsed XPAL system have also been modeled by Palla *et al.* [Palla, 2010]. A more detailed discussion of XPAL, as well as differences and similarities to DPAL systems may be found in [Readle 2008, 2009a-b, 2010a-b; Heaven, 2010; Galbally-Kinney, 2010]. In this paper we discuss further high fidelity modeling results from BLAZE-V and a simple theoretical model to investigate the expected conditions to reach optical transparency in different gas mixtures and temperatures.

2. BLAZE-V DETAILED MODELING

The multi-physics BLAZE-V model [Palla, 2010] was updated and employed for more detailed studies in the past year. BLAZE-V is a multi-dimensional, transient, finite-volume, plasma-kinetic, fluid-dynamic model and was adapted and extended to model time-dependent specie molecular continuity, including kinetics and diffusion, energy conservation, and radiation transport including interaction with the gain media and boundaries over a two or three-dimensional computational domain appropriate to a non-flowing XPAL configuration. The model is capable of generating and solving appropriate Cartesian (structured) and unstructured grids. The model uses a kinetic set including nine species: Ar, Cs($6^2S_{1/2}$), Cs($6^2P_{1/2}$), Cs($6^2P_{3/2}$), CsAr($X^2\Sigma^+_{1/2}$), CsAr($A^2\Pi_{1/2}$), CsAr($A^2\Pi_{3/2}$), CsAr($B^2\Sigma^+_{1/2}$), and C₂H₆. All relevant thermodynamic data for the included species is contained in the model. The model contains the following 12 reactions for four- and five-level XPAL calculations:



The Cs + Ar ↔ CsAr association and dissociation rate constants were estimated [Palla, 2010] using the quasi-static approximation and a simple collision frequency model. Other rates for Cs were taken from Beach *et al.* [Beach, 2004] and Steck [Steck, 2003].

The BLAZE-V model was thoroughly baselined to both four- and five-level pulsed XPAL data in earlier studies [Palla, 2010] and herein we begin to perform calculations to help guide future experiments.

2.1 Pulsed XPAL calculations as a function of temperature

One of the early questions for XPAL is the effect of temperature on performance. From the experimental data [Readle, 2009a; Readle, 2010b] it was clear that increased temperature would simultaneously increase the pump energy required for lasing threshold, but we wanted to know if there were any particular benefits to higher cell temperatures in terms of performance in the pulsed system.

These parametric studies were performed assuming *four-level* operation using the 837 nm pump pathway and lasing at 852 nm, Figs. 3 and 4. No ethane was present in these calculations. For enhanced calculation speed, a pump pulse with a radially symmetric Gaussian profile and a full-width at half-maximum (FWHM) radius value of 0.18 cm was used in place of the elliptically shaped beam of the experiments. The pump pulse had a temporal Gaussian profile with a FWHM value of 4.3 ns. Calculated outcoupled laser energy as a function of absorbed pump energy results are in good agreement with the 10-cm cell length data [Readle, 2010b], Fig. 5. Note that the model predicts a slightly higher absorbed energy threshold of approximately 150 μJ for this case, Fig. 5, compared to approximately 130 μJ for the data [Readle, 2010a]. As a function of temperature, the calculations show the anticipated trend of higher laser threshold energy for higher temperature in proportion to the Cs vapor pressure rise with temperature, Fig. 5.

Calculations were performed for considerably higher absorbed energies, Fig. 6. The outcoupled laser energies begin to flatten for the lower temperature cases of 414 K and 464 K. This is a result of there being a limit to the rate at which energy can be absorbed by the Cs-Ar collision pairs based upon the actual number density of Cs. With higher temperature one is able to couple in more energy, and subsequently outcouple more laser energy simply based upon the higher number density of Cs. However, the largest slopes at each temperature are similar, therefore the initial conclusion is that the efficiency of the pulsed XPAL system does not change substantially with temperature.

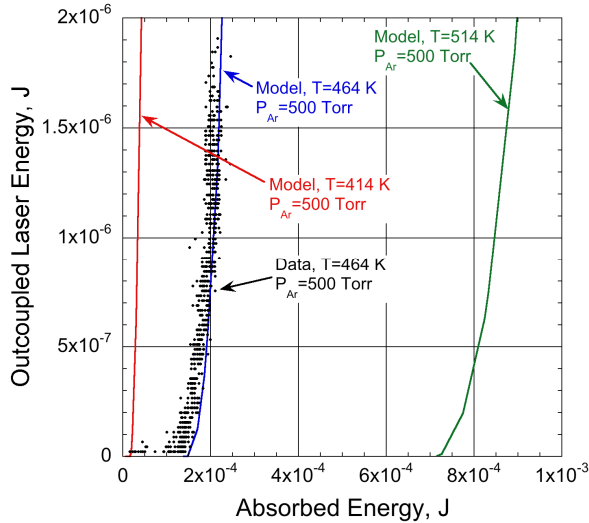


Figure 5. BLAZE-V predictions of outcoupled laser energy vs. absorbed energy as a function of cell temperature with a comparison to pulsed data at 464 K [Readle, 2010b].

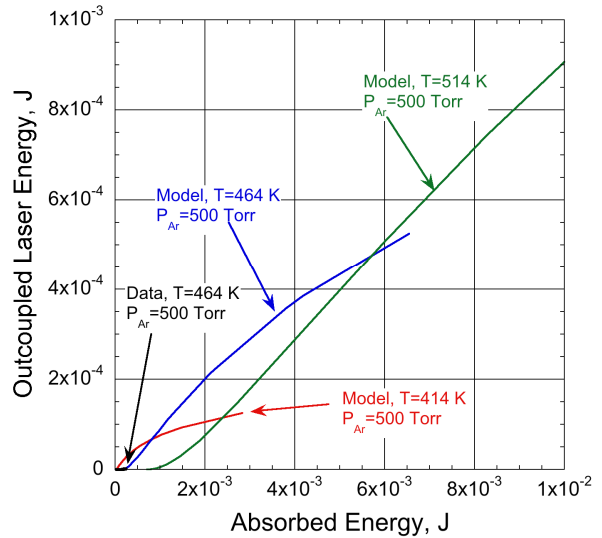


Figure 6. BLAZE-V predictions of outcoupled laser energy vs. absorbed energy as a function of cell temperature with a comparison to pulsed data at 464 K [Readle, 2010b] on an expanded scale. (Note: data is barely visible in the lower left corner of the plot.)

The time evolution of the upper and lower laser level Cs states' concentrations (not shown for brevity) are consistent with theory as they reach values with a ratio near to the ratio of their respective statistical weights while lasing. As a function of the cell temperature these concentrations change in magnitude, but are qualitatively the same as shown previously by Palla *et al.* [Palla, 2010].

2.2 Pulsed XPAL calculations as a function of rare gas pressure

Another early question for XPAL is the effect of rare gas pressure on performance. These parametric studies were also performed assuming *four-level* operation using the 837 nm pump pathway and lasing at 852 nm, Figs. 3 and 4. No ethane was present in these calculations. For enhanced calculation speed, a pump pulse with a radially symmetric Gaussian profile and a full-width at FWHM radius value of 0.18 cm was used in place of the elliptically shaped beam of the experiments. The pump pulse had a temporal Gaussian profile with a FWHM value of 4.3 ns. For these calculations the cell temperature was fixed at 464 K.

Calculated outcoupled laser energy versus absorbed pump energy as a function of the rare gas cell pressure are shown in Figs. 7 and 8. The data points are the same as shown in Fig. 5, but on a more close up scale. BLAZE-V predicts that the threshold for lasing shifts slightly towards a lower threshold for higher rare gas pressure. Larger rare gas pressure will result in more collision pairs, which will consequently result in a larger overall amount of energy absorbed. However, Fig. 7 is plotted as a function of absorbed energy, so it is not immediately clear why the threshold would shift slightly with increased pressure. From reaction *R.5*, it is possible that the 3-body collisions create more population of the CsAr($A^2\Pi_{3/2}$) state that can act as a small reservoir of energy for feeding the Cs($6^2P_{3/2}$); this may account for a small shift towards lower threshold energy at higher rare gas pressure. Figure 8 shows that there are significant advantages to having a higher rare gas pressure as more power is absorbed by the gain medium; this may also be related to the 3-body

collisions creating an energy reservoir in the CsAr($A^2\Pi_{3/2}$) state, but needs to be investigated further to better understand this effect.

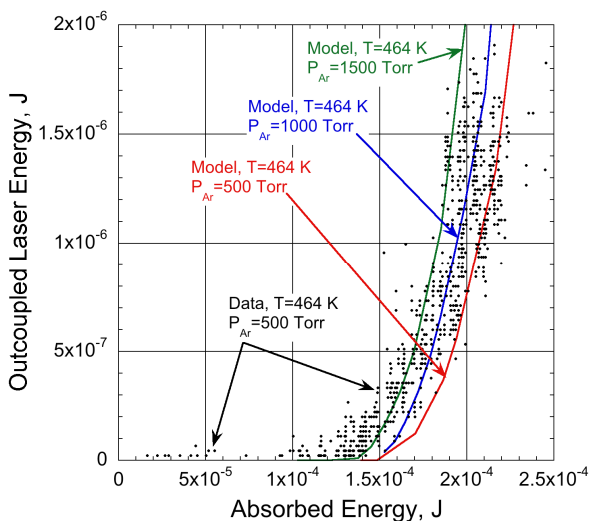


Figure 7. BLAZE-V predictions of outcoupled laser energy vs. absorbed energy as a function of rare gas pressure with a comparison to pulsed data at 464 K [Readle, 2010b].

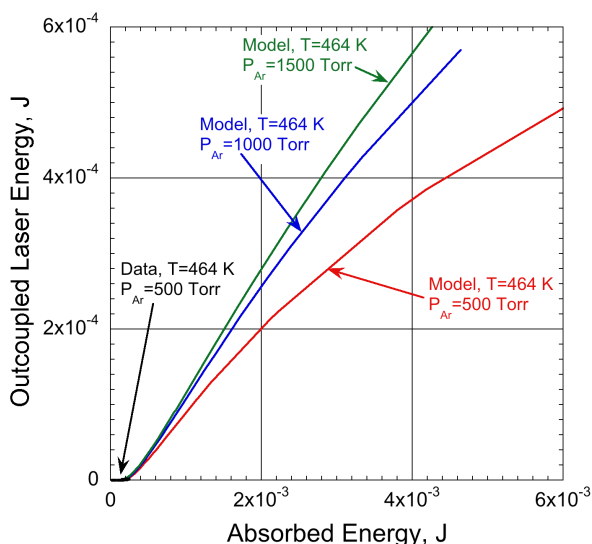


Figure 8. BLAZE-V predictions of outcoupled laser energy vs. absorbed energy as a function of rare gas pressure with a comparison to pulsed data at 464 K [Readle, 2010b] on an expanded scale. (Note: data is barely visible in the lower left corner of the plot.)

Preliminary computations with an amplified spontaneous emission (ASE) model (not shown for brevity) indicated that there was no significant parasitic lasing mechanism for the pulsed beam experiments discussed above [Palla, 2010]. Further study using the ASE model is suggested for higher pump volume system configurations in which more significant ASE effects may be possible.

3. PRELIMINARY THEORETICAL MODEL

To enable quick studies for cw performance, a preliminary analytic model was created for the four-level XPAL system. Assumptions in the theory include:

- (i) that the equilibrium between the Cs($6^2S_{1/2}$) and CsAr($X^2\Sigma^+_{1/2}$) states is maintained in steady-state lasing,
- (ii) that the equilibrium between the Cs($6^2P_{3/2}$) and CsAr($B^2\Sigma^+_{1/2}$) states is maintained in steady-state lasing,
- (iii) the CsAr($A^2\Pi_{1/2}$) and CsAr($A^2\Pi_{3/2}$) states do not play a significant role,
- (iv) the Cs($6^2P_{1/2}$) state does not play a significant role in the four-level system,
- (v) and spontaneous emission from the CsAr($B^2\Sigma^+_{1/2}$) state is neglected.

The species in the model are denoted as: N_0 for Cs($6^2S_{1/2}$), N_1 for CsAr($X^2\Sigma^+_{1/2}$), N_2 for CsAr($B^2\Sigma^+_{1/2}$), N_3 for Cs($6^2P_{3/2}$), and M for Ar, Fig. 9. Note that the precise species of alkali and rare gas can be replaced by other alkalis or rare gases,

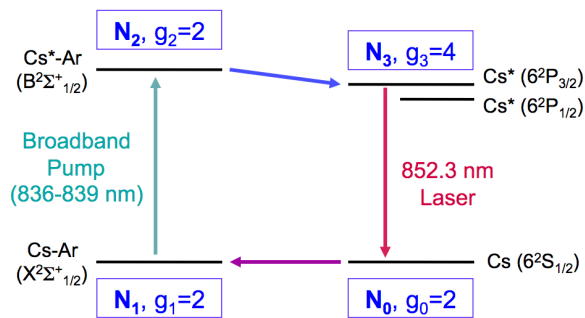


Figure 9. Schematic of the energy levels and number densities N_i considered in the four-level XPAL theoretical model.

e.g., one could use Rb in place of Cs, and Kr in place of Ar. First we define the equilibrium fractions f_{10} and f_{23} , which provide relations between N_1 and N_0 , and N_2 and N_3 :

$$f_{10} = \frac{N_1}{N_0} = \frac{\left[\text{CsAr}(X^2\Sigma_{1/2}) \right]}{\left[\text{Cs}(^2S_{1/2}) \right]} = \frac{g_1}{g_0} 4\pi R_0^2 \Delta R \exp\left(\frac{-\Delta E_{10}}{k_b T}\right) [M] \quad E.1$$

$$f_{23} = \frac{N_2}{N_3} = \frac{\left[\text{CsAr}(B^2\Sigma_{1/2}) \right]}{\left[\text{Cs}(^2P_{3/2}) \right]} = \frac{g_2}{g_3} 2\pi R_0^2 \Delta R \exp\left(\frac{-\Delta E_{23}}{k_b T}\right) [M] \quad E.2$$

where k_b is the Boltzmann constant, R_0 is the optimal internuclear separation (4.5 Å for Cs-Ar) for the blue satellite, ΔR is the range of distances over which the resonance absorption condition is maintained (1 Å), and $[M]$ is the rare gas concentration. Note that R_0 and ΔR are implicitly dependent on the bandwidth of the excitation source. These expressions come from quasi-static approximations for the collision pairs as done by [Hedges, 1972] and [Eden, 1976]. The factor of 2 difference in *E.2* arises because collisions between Cs($6^2P_{3/2}$) and Ar sample both the $B^2\Sigma_{1/2}^+$ and $A^2\Pi_{3/2}$ potential energy curves [Palla, 2010]. The exponential terms in *E.1* and *E.2* involve ΔE_{ij} , which is the difference in the potential energy between the collision pair state at R_0 and the unbound state at $R = \infty$, and are defined by

$$\Delta E_{10} = U_1(R = R_0) - U_0(R = \infty) \quad E.3$$

$$\Delta E_{23} = U_2(R = R_0) - U_3(R = \infty) \quad E.4$$

At the peak of the blue satellite (4.5 Å), the CsAr($X^2\Sigma_{1/2}^+$) potential is very slightly repulsive, $\Delta E_{10} = 10 \text{ cm}^{-1}$ [Merritt, 2009], and the CsAr($B^2\Sigma_{1/2}^+$) potential is entirely repulsive, such that $\Delta E_{23} = 249 \text{ cm}^{-1}$ at $R_0 = 4.5 \text{ Å}$.

We further know that the sum of the Cs containing species must obey conservation, therefore

$$N_T = N_0 + N_1 + N_2 + N_3 \quad E.5$$

Under lasing conditions the threshold gain g_{th} is defined by the gain-equals-loss relation

$$g_{th} = -\frac{1}{2L_g} \ln(r_1 r_2) = \sigma_{30} [N_3 - 2N_0] \quad E.6$$

where L_g is the gain length, r_i are the mirror reflectivities, and the factor of 2 multiplier to N_0 is a result of the degeneracy ratio g_3/g_0 between the upper and lower states of the four-level system. The system of equations *E.1* – *E.6* can be solved to find the number densities of the species in the cw threshold lasing case to be:

$$N_0 = \frac{N_T - (1 + f_{23})g_{th} / \sigma_{30}}{3 + f_{10} + 2f_{23}} \quad E.7$$

$$N_3 = \frac{g_{th}}{\sigma_{30}} + 2N_0 \quad E.8$$

$$N_1 = f_{10}N_0 \quad E.9$$

$$N_2 = f_{23}N_3 \quad E.10$$

At conditions for optical transparency (OT), the gain is zero and therefore Eqs. *E.7* and *E.8* reduce to,

$$N_{0,OT} = \frac{N_T}{3 + f_{10} + 2f_{23}} \quad E.11$$

$$N_{3,OT} = 2N_{0,OT} \quad E.12$$

For a Cs-Ar laser with $r_1=0.50$ and $r_2=1.0$, the number densities of the different species $N_0 - N_3$ are shown in Fig. 10. Note that this simple analytical approach predicts number densities at 464 K of $N_0=4.24 \times 10^{14}$, $N_1=2.36 \times 10^{12}$, $N_2=1.59 \times 10^{12}$, and $N_3=8.48 \times 10^{14}$, which are very similar to the values predicted by the detailed BLAZE-V model [Palla, 2010].

One of the challenges for XPAL will be to properly absorb the broadband pump radiation on the $N_2 \leftarrow N_1$ ($B \leftarrow X$) transition and a multi-pass pump configuration may be required. Using Beer's Law, one can make an estimate of how many passes would be required to absorb 90% of the pump radiation. If we make the assumption that we would like 1-10 passes in a 10 cm cell, Fig. 11 shows that our operating range should likely be at a temperature of 450-550 K.

An analytical rate equation approach can be used to better understand the expected laser output as a function of pump input. Preliminary work with the rate equations (not shown for brevity) provides the following for the pump intensity for optical transparency (OT, gain=0) inside the gain volume:

$$I_{P,OT} = \frac{2h\nu_P}{\sigma_P \tau_3 (f_{10} - 2f_{23})} \quad E.13$$

where σ_P is the cross-section for the pump beam, I_P is the intensity of the pump beam in the cell volume, ν_P is the frequency of the pump beam, and τ_3 is the spontaneous emission lifetime of the upper state. Note that *E.13* actually represents the "intracavity" or "gain volume" pump intensity that builds up in a multi-pass cell (whereas it may be possible to actually pump or "feed" the cell with considerably lower intensity).

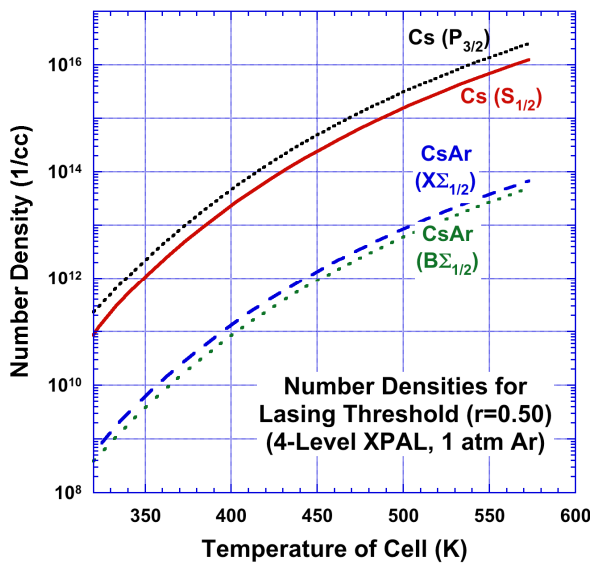


Fig. 10. Number densities N_i predicted by the four-level XPAL theoretical model under threshold lasing conditions using a 50% outcoupler.

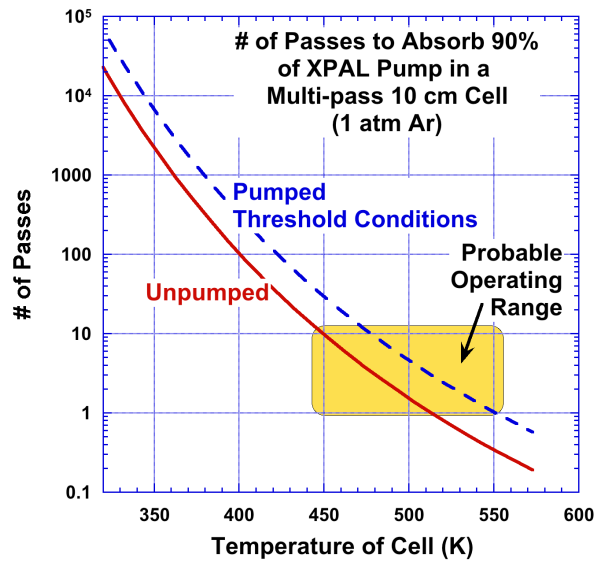


Fig. 11. Number of passes required to absorb 90% of pump power predicted by the four-level XPAL theoretical model.

A check on the accuracy of the theoretical model can be obtained by comparing to data, however we only have pulsed data available [Readle, 2010b] and our theory is designed for steady-state operation. Nevertheless, we can make some estimates by recognizing that (i) the number density required for optical transparency is defined by *E.12* and *E.11*, and (ii) because the energy absorbed by the exciplex is rapidly transferred to the $P_{3/2}$ state, the number density of the $P_{3/2}$ state to first-order defines the amount of energy that must be absorbed for a specified pulse time τ_{pulse} and interacting gas volume (FWHM area of pump beam multiplied by length of gas cell), $V = A_P L_{cell}$. The energy absorbed by the gas medium can thus be estimated as

$$E_{abs,OT} \cong h\nu_P N_{3,OT} A_P L_{cell} \tau_{pulse} \quad E.13$$

Using *Eqs. 11 – 12* and *13*, we can now make a direct comparison between our preliminary theory and the experimental data of Readle *et al.* [Readle, 2010b], Fig. 12; the theory is in reasonable agreement with data as a function of gas cell temperature and provides some confidence in the model.

In previous modeling [Palla, 2010] we have noted that intensities on the order of 10^6 W/cm² are required to achieve optical transparency in a CsAr XPAL, which raises the question: are there other alkali and rare gas mixtures that are more favorable in terms of the required pump intensity? To answer this question we need to have measurements of the

absorption of the collision pair, for which data is sparse. Chen and Phelps [Chen, 1973] established a solid value of the reduced absorption coefficient of $1.3 \times 10^{-36} \text{ cm}^5$ at 837 nm for CsAr and this was confirmed by measurements using modern instrumentation by Readle [Readle, 2010c]. Galbally-Kinney et al. [Galbally-Kinney, 2010] provide transmission data for a Rb-Kr gas mixture, and we extract a value of $1.66 \times 10^{-36} \text{ cm}^5$ from this data for the reduced absorption coefficient at 758 nm. However, we note that very little other transmission as a function of wavelength (blue satellite) data appears in the literature for alkali – rare gas mixtures. Blue satellite absorption data exist for Cs-Kr [Readle, 2010c], Cs-Xe [Eden, 1976; Readle, 2010c], Cs-Ar-Kr [Readle, 2010c], and mixtures that include an absorption enhancer such as ethane [Galbally-Kinney, 2010; Readle, 2010c]. While calculations can be made to provide estimates of these absorption coefficients [Baylis, 1969; Heaven, 2010; Readle, 2010c], the theoretical predictions appear to be good to only within a factor of $2 \times$ and therefore we recommend that more absorption measurements are needed for other alkali – rare gas mixtures to better understand which gas mixtures will be most suitable for scaling.

To get an idea of whether other gas mixtures can be useful, we compare the predicted pump intensity for optical transparency for Cs-Ar and Rb-Kr mixtures, Fig. 13. For these calculations the peak of the blue satellite for RbKr is at 4.4 \AA [Heaven, 2010], the RbKr($X^2\Sigma^+_{1/2}$) potential is very slightly attractive, $\Delta E_{10} = -25 \text{ cm}^{-1}$, and the RbKr($B^2\Sigma^+_{1/2}$) potential is repulsive with $\Delta E_{23} = 444 \text{ cm}^{-1}$ at $R_0=4.5 \text{ \AA}$ [Heaven, 2010]. Clearly Rb-Kr appears to have a significantly lower required pump intensity than does Cs-Ar, thereby suggesting that this mixture and possibly others may be better candidates for a scaled cw XPAL system.

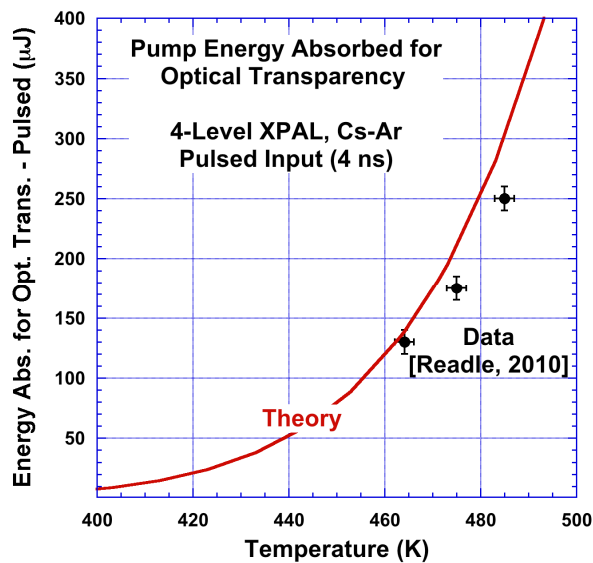


Fig. 12. Energy absorbed to reach optical transparency in pulsed operation; comparison between theory and data of Readle *et al.* [Readle, 2010b].

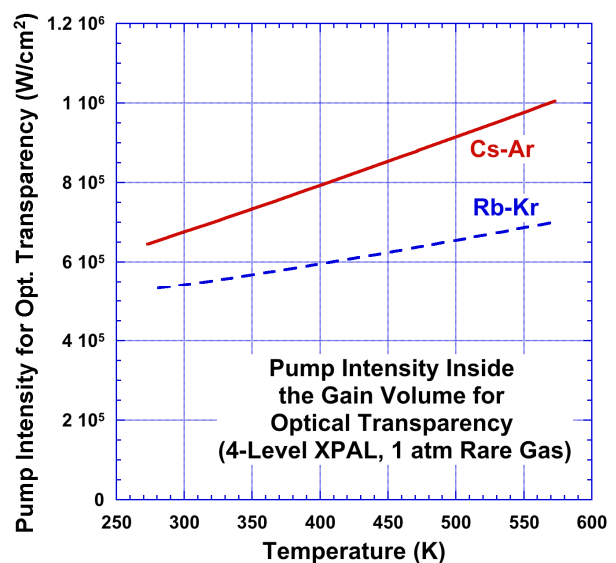


Fig. 13. Pump intensity required for optical transparency predicted by the four-level XPAL theoretical model for Cs-Ar and Rb-Kr mixtures.

The results shown in Fig. 13 raise the question: what are the driving factors for the lower pump intensity required for Rb-Kr mixtures? The factors that influence I_p in *E.13* are τ_3 , ν_p , σ_p , f_{10} , and f_{23} . τ_3 is 30.5 ns for Cs and 26.24 ns for Rb, which actually increases I_p for Rb by $\approx 16\%$. ν_p is 837 nm for Cs-Ar and 758 nm for Rb-Kr, so this represents a 10% drop in I_p . At 200°C , σ_p is $6.5 \times 10^{-15} \text{ cm}^2$ for Cs-Ar and $6.8 \times 10^{-15} \text{ cm}^2$ for Rb-Kr, so this results in approximately a 5% drop in I_p . Essentially the net of these three factors is no change in I_p , therefore the key factor(s) must be f_{10} , and/or f_{23} . To examine these factors, they are plotted as a function of temperature in Fig. 14. Several things become clear:

- 1) f_{10} for Rb-Kr is larger than Cs-Ar indicating that there will be a greater concentration of the ground state Rb-Kr collision pair. This makes sense since the Rb-Kr pair is slightly attractive ($\Delta E_{10} = -25 \text{ cm}^{-1}$) in the blue satellite whereas the Cs-Ar pair is slightly repulsive ($\Delta E_{10} = 10 \text{ cm}^{-1}$). A larger concentration of the collision pair enables a larger absorption of the pump, i.e., faster pumping to the exciplex.
- 2) f_{23} for Rb-Kr is smaller than Cs-Ar indicating that there will be a smaller concentration of the exciplex state of Rb-Kr. This makes sense since the Rb-Kr exciplex is more repulsive ($\Delta E_{23} = 444 \text{ cm}^{-1}$) than the Cs-Ar exciplex

($\Delta E_{23} = 249 \text{ cm}^{-1}$) therefore the Rb-Kr exciplex will break apart more rapidly. Faster dissociation of the exciplex provides rapid transfer of energy into the desired upper laser level and helps to prevent the pumping from overwhelming the dissociation rate.

- 3) The factor of $(f_{10} - 2f_{23})$ in the denominator of $E.13$ indicates that the effect of f_{23} is further amplified by a factor of $2\times$, therefore the f_{23} factor becomes the more dominant term.
- 4) Figure 15 illustrates that the factor $(f_{10} - 2f_{23})$ for Rb-Kr is significantly larger than that for Cs-Ar and this quantity is the primary reason why the required pump intensity for Rb-Kr is lower, Fig. 13. Note that I_p is inversely proportional to $(f_{10} - 2f_{23})$, therefore as $(f_{10} - 2f_{23})$ decreases I_p will increase.

These result suggest that through proper choice of the alkali – rare gas pair, it may be possible to significantly reduce the required pump intensities for the XPAL system and thereby enable a more scalable device. It is noted that a mixture of multiple rare gases, as done by Readle et al. [Readle, 2010b; Readle, 2010c], may further enhance results by broadening the blue satellite.

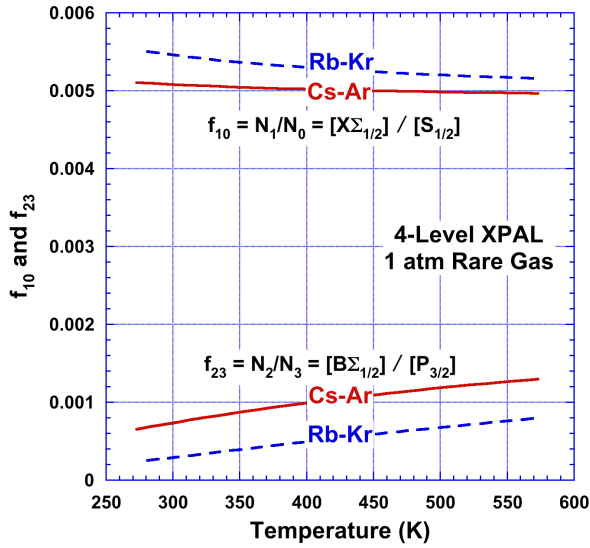


Figure 14. Predicted values of f_{10} and f_{23} as a function of cell temperature for Cs-Ar and Rb-Kr.

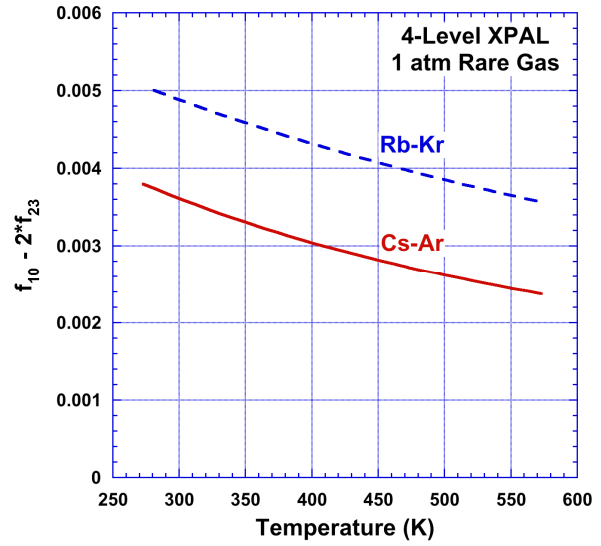


Figure 15. Predicted values of $f_{10} - 2f_{23}$ as a function of cell temperature for Cs-Ar and Rb-Kr.

5. CONCLUDING REMARKS

The BLAZE-V model was utilized for high-fidelity simulations. BLAZE-V is a time-dependent finite-volume model including transport, thermal, and kinetic effects appropriate for the simulation of a cylindrical closed cell XPAL system. The model is also regularly used for flowing gas laser simulations and is easily adapted for DPAL. The detailed BLAZE-V modeling predicts higher XPAL performance as the rare gas pressure increases, and that higher output powers are obtainable with higher temperature. The preliminary theory is in reasonable agreement with experimental optical transparency data as a function of gas cell temperature. Rb-Kr appears to have significantly lower required pump intensity than does Cs-Ar, thereby suggesting that this mixture and possibly others may be better candidates for a scaled cw XPAL system. Thus, we recommend that more absorption measurements are needed for other alkali – rare gas mixtures to better understand which gas mixtures will be most suitable for scaling. The future simulation effort using the BLAZE-V and theoretical models will continue to refine and expand the capabilities of the code and theory, while at the same time expanding the predictions to help guide future experiments with long term scaling of the system in mind.

ACKNOWLEDGMENTS

This work was supported by the Joint Technology Office through the U.S. Air Force Office of Scientific Research (AFOSR) under contract number FA9550-07-1-0575. The authors gratefully thank: J.G. Eden, C.J. Wagner, D. Hewitt,

and T. Houlahan (Univ. of Illinois at Urbana-Champaign); W. T. Rawlins and S. J. Davis (Physical Sciences Inc.); and M. Berman (AFOSR).

REFERENCES

- Baylis, W.E., *J. Chem. Phys.*, **51**, 2655 (1969).
- Beach, R. J., Krupke, W. F., Kanz, V. K., and Payne, S. A., *J. Opt. Soc. Am. B*, **21**, pp. 2151-2163 (2004).
- Chen, C. L., and Phelps, A. V., *Phys. Rev. A*, **7**, 470, (1973).
- Eden, J.G., Cherrington, B.E., and Verdeyen, J.T., *IEEE J. Quant. Elect.*, **QE-12**, 698 (1976).
- Galbally-Kinney, K.L., Kessler, W.J., Rawlins, W.T., and Davis, S.J., "Spectroscopic and Kinetic Measurements on Alkali Atom-Rare Gas Excimers," AIAA Paper 2010-5044 (2010).
- Hager, G.D., and Perram, G.P., *Appl. Phys. B: Lasers and Optics*, **101**, 45-56 (2010).
- Heaven, M.C., and Stolyarov, A.V., "Potential Energy Curves for Alkali Metal – Rare Gas Exciplex Lasers," AIAA Paper 2010-4877 (2010).
- Hedges, R. E. M., Drummond, D. L., and Gallagher, A., *Phys. Rev. A*, **6**, 1519 (1972).
- Komashko, A.M., and Zweiback, J., "Modeling laser performance of a scalable side pumped alkali laser," SPIE Vol. **7581**, 75810H (2010).
- Krupke, W. F., Beach, R. J., Kanz, V. K., and Payne, S. A., *Opt. Lett.*, **28**, 2336 (2003).
- Krupke, W. F., Beach, R. J., Kanz, C. K., and Payne, S. A., *Proc. SPIE* **5334**, 156 (2004).
- Merritt, J. M., Han, J., Chang, T., and Heaven, M. C., "Theoretical investigations of alkali metal – rare gas interaction potentials," Proc. SPIE, 7196, 71960H (2009).
- Palla, A. D., Carroll, D. L., Verdeyen, and Heaven, M. C., "Multi-Dimensional Modeling of the XPAL System," AIAA Plasmadynamics and Lasers Conference, Chicago, Illinois, June 2010, AIAA Paper 4878–2010 (2010).
- Podvyaznyy, A., Venus, G., Smirnov, V., Mokhun, O., Koulechov, V., Hostutler, D., and Glebov, L., "250W diode laser for low pressure Rb vapor pumping," *SPIE* **7583**, 758313 (2010).
- Readle, J. D., Wagner, C. J., Verdeyen, J. T., Carroll, D. L., and Eden, J. G., *Electronics Letters*, **44**, 25 (2008).
- Readle, J. D., Wagner, C. J., Verdeyen, J. T., Spinka, T. M., Carroll, D. L., and Eden, J. G., *Appl. Phys. Lett.*, **94**, 251112 (2009a).
- Readle, J. D., Wagner, C. J., Verdeyen, J. T., Carroll, D. L., and Eden, J. G., "Lasing in alkali atoms by the dissociation of alkali-rare gas exciplexes (excimers)," *SPIE* **7196**, 71960D (2009b).
- Readle, J. D., Wagner, C. J., Verdeyen, J. T., Spinka, T. M., Carroll, D. L., and Eden, J. G., "Excimer-pumped alkali vapor lasers: A new class of photoassociation lasers," SPIE Vol. **7581**, 75810K (2010a).
- Readle, J. D., Eden, J. G., Verdeyen, J. T., and Carroll, D. L., *Appl. Phys. Lett.*, **97**, 021104 (2010b).
- Readle, J.D., "Atomic Alkali Lasers Pumped by the Dissociation of Photoexcited Alkali-Rare Gas Collision Pairs," Ph.D. Dissertation, University of Illinois at Urbana-Champaign (2010c).
- Steck, D. A., "Cesium D line data," available online at <http://steck.us/alkalidata> (2003).
- Zhdanov, B., et al., *Optics Comm.* **270**, 353 (2007a).
- Zhdanov, B.V., and Knize, R.J., *Elect. Lett.* **43**, 1024 (2007b).
- Zhdanov, B. V., Sell, J., and Knize, R. J., *Electron. Lett.*, **44**, 582 (2008).
- Zweiback, J., Hager, G., and Krupke, W.F., *Opt. Comm.* **282**, 1871 (2009).
- Zweiback, J., Komashko, A., and Krupke, W.F., "Alkali vapor lasers," SPIE Vol. **7581**, 75810G (2010).